

See discussions, stats, and author profiles for this publication at: <https://www.researchgate.net/publication/231240918>

pH-Responsive Bridged Silsesquioxane

ARTICLE *in* CHEMISTRY OF MATERIALS · MARCH 2011

Impact Factor: 8.35 · DOI: 10.1021/cm103327y

CITATIONS

10

READS

38

5 AUTHORS, INCLUDING:



[Laurent Fertier](#)

EcoLogicSense

10 PUBLICATIONS 50 CITATIONS

[SEE PROFILE](#)



[Christophe Theron](#)

University of New Mexico

6 PUBLICATIONS 25 CITATIONS

[SEE PROFILE](#)



[Philippe Trens](#)

Ecole Nationale Supérieure de Chimie de Mo...

82 PUBLICATIONS 1,196 CITATIONS

[SEE PROFILE](#)



[Michel Wong Chi Man](#)

French National Centre for Scientific Research

188 PUBLICATIONS 3,577 CITATIONS

[SEE PROFILE](#)

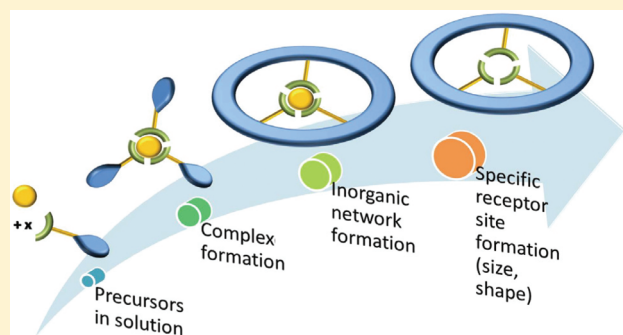
pH-Responsive Bridged Silsesquioxane

Laurent Fertier, Christophe Théron, Carole Carcel,* Philippe Trens, and Michel Wong Chi Man*

ICG Montpellier (UMR 5253) CNRS-UMII-ENSCM-UMI, 8 rue de l'école normale, 34296 Montpellier CEDEX 5, France

 Supporting Information

ABSTRACT: A pH-responsive bridged silsesquioxane was obtained via the sol–gel process from a bis-silylated triazine derivative bearing a triple DAD (donor–acceptor–donor) moiety which was strongly hydrogen-bonded to the three ADA (acceptor–donor–acceptor) sites of cyanuric acid. The latter template molecule was easily removed from the resulting hybrid material upon acidic treatment, which yielded the template-free bridged silsesquioxane with preserved morphology and unaltered particle size as demonstrated by SEM. As expected, the surface area of the acid-treated hybrid was significantly higher than that of the untreated material, as demonstrated by nitrogen adsorption measurements. The absence of cyanuric acid in this material was confirmed by solid state NMR and by IR. It was shown that a mild acidic medium ($\text{pH} = 5.5$) is sufficient to release the cyanuric acid template, thus providing a novel route to new hybrid materials with potential applications as efficient carriers for pH-responsive delivery systems.



KEYWORDS: bridged silsesquioxanes, molecular recognition, pH-responsive hybrid silica, imprinting

INTRODUCTION

In recent years, significant effort has been focused toward the synthesis of porous materials with potential applications such as for drug-delivery carriers^{1–3} and for catalysis.⁴ These materials consist of either organic or inorganic polymers,^{5,6} among which silica meets most of the requirements as a good support: chemical inertness, thermal and mechanical stability, and also the possibility of tailoring the size and the shape of the pores and cavities inside the materials.^{7–9} Mesoporous materials were obtained using surfactants as structuring agents and from this surfactant-mediated route, organic groups may be covalently anchored in two ways: (1) grafting a functional alkoxy silane on a preformed mesoporous silica (MCM- or SBA-type); and (2) co-condensation of the functional alkoxy silane with TEOS in the presence of a suitable surfactant.^{10–12} Following these two methods, many forms of functional mesoporous hybrids have been synthesized and exploited for many applications.¹³ For example, mechanized nanomachines have been prepared for on-demand release of cargo molecules (including drugs, dyes, biomolecules, etc.)¹⁴ as well as easily recoverable and recyclable homogeneous catalysts supported on hybrid porous silicates which have applications in a variety of chemical processes.¹⁵ Hybrid mesoporous silica can also be prepared via the self-assembly of organopolysilane precursors bearing a long alkylene chain. In this case, self-structuring occurs to form a purely hybrid silica without added TEOS and without any surfactant.^{16,17} Complementary to these are the periodic mesoporous organosilicates (PMO) obtained from bridged silsesquioxane precursors, which are prepared with surfactants.^{18,19} In the series of bridged silsesquioxanes, labile Si–C covalently bonded ethynyl units were softly cleaved by a chemical route to

afford mesoporous silica.²⁰ The pore sizes and distribution were dependent on both the structure of the sacrificial ethynyl templates and the reaction conditions employed.²¹

Porous materials can also be obtained by molecular imprinting techniques which are used to create solid materials containing chemical functionalities that are spatially localized and fixed by interactions with the imprint molecules during the synthesis process. Subsequent removal of these template molecules leaves preformed sites for the recognition of small molecules, hence affording materials which may be suitable for applications in separation chemistry.²² Indeed, protein-imprinted silica prepared via covalent imino group bonding showed enhanced affinity for the template protein compared to the corresponding imprinted silica obtained by entrapment of the protein with no interaction of the latter with the silica surface.²³ Using a chiral cationic surfactant in conjunction with sol–gel processing, chiral imprinted silica-based thin films were obtained, which exhibited good selectivity toward chiral alcohols.²⁴ Imprinted polysilsesquioxanes have also been obtained by the co-condensation of a bridged organosilane (BTSE) precursor with *N*-[3-(trimethoxysilyl)propyl]ethylene-diamine (TMS(en)) in the presence of several cations (CuII, ZnII, and NiII). The removal of these cations created cavities within the hybrids which exhibited selective rebinding characteristics.²⁵ More recently we described imprinted hybrid silicas (IHS), in which the covalently bonded molecular recognition sites in the inorganic matrix were templated with the complementary imprint

Received: November 19, 2010

Revised: March 16, 2011

Published: March 31, 2011

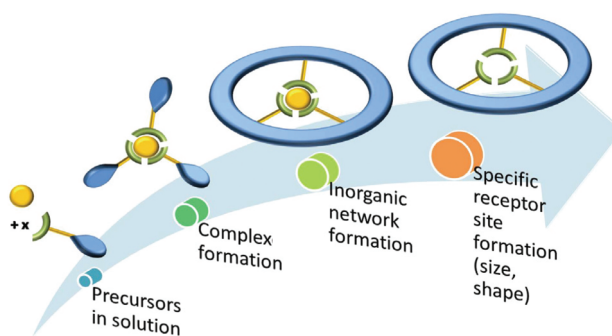


Figure 1. Imprinted hybrid silica preparation.

molecule.²⁶ The removal of the latter organic imprint is expected to leave specific receptor sites with tightly controlled dimensions and shapes under mild processing conditions (Figure 1). The formation of a complex involving multiple hydrogen bonds between the initially confined template and the matrix enables this system to be controlled by an external stimulus, namely the pH, since an acidic environment causes the rupture of the hydrogen bonds, and associated release of the template molecule. This was demonstrated with a monosilylated precursor, (triethoxysilyl)-propylcyanurate having two ADA recognition faces which can easily complex melamine.²⁶ A hybrid silica material was thus obtained by co-condensation of TEOS with the silyl derivative hydrogen-bonded to pure melamine as template to imprint the material. In this case, the melamine was completely removed under strong acidic treatment ($\text{pH} = 2$). It was shown that melamine could be subsequently reintroduced quantitatively, after pretreating the template-free hybrid with triethylamine, although the resulting materials exhibited some textural modifications. Bridged silsesquioxanes^{27,28} are more suitable than the hybrid silicas obtained by the co-condensation method, as the exclusion of TEOS enables more organic species to be tethered to the rigid framework, as well as a higher loading of the template molecule in the resulting hybrid silica.

The objective of this work is to use molecular imprinting^{29,30} via weak H-bonds to create bridged silsesquioxanes containing chemical functionalities that can release the imprint (or template) molecules under mild acidic activation conditions. Herein, we report the synthesis of a pH-responsive bridged silsesquioxane obtained from a bis-silylated triazine derivative, bearing only one DAD (donor–acceptor–donor) face and two hydrolyzable trialkoxysilyl groups, associated with cyanuric acid through H-bonding. Removal of the cyanuric acid under strong acidic condition was studied and the possibility of using this bridged silsesquioxane as a potential carrier to release cyanuric acid at 37°C at moderate pH was also examined.

EXPERIMENTAL SECTION

General Methods. The synthesis of the silylated molecular precursor was carried out in an inert atmosphere and by using vacuum line and standard Schlenk techniques. The reagents were used as received. The solvents were dried using MB SPS-800 apparatus. The melting points were determined on Büchi Melting Point B-540 and are uncorrected. The FTIR data were obtained on a Perkin-Elmer FT-IR system Spectrum BX spectrophotometer equipped with GladiaATR. Liquid ^1H and ^{13}C NMR spectra were recorded on a Bruker AC-400 spectrometer at room temperature with CDCl_3 as the solvent and tetramethylsilane (TMS) as an internal reference. Solid state ^{13}C and ^{29}Si NMR spectra were obtained

using a Bruker FT-AM 400 spectrometer using cross-polarization and magic-angle spinning techniques (CP-MAS). The high-resolution mass spectra (Q-TOF ES+) were measured on a JEOL MS-DX 300 mass spectrometer. Discontinuous nitrogen sorption isotherms were measured at 77.15 K using a Micromeritics 2010 apparatus. Specific surface areas were derived using the BET transform of the sorption isotherms, taking 0.162 nm^2 as the cross section area for nitrogen.³¹ No microporosity could be detected using the t-plot method, taking Aerosil200 as reference.³² TGA analyses were performed on a TA Instruments ATG Q50 from 25° to 500°C , with a ramp rate of $10^\circ\text{C}/\text{min}$.

Synthesis. Compound **1** (*2-N,N-bis(2-Cbz-Aminoethyl)amino-4,6-dichloro-1,3,5-triazine*). 2,4,6-Trichloro-1,3,5-triazine (0.478 g, 2.59 mmol) was dissolved in THF (20 mL) and the resulting solution cooled in a water/ice bath before adding diisopropylethylamine (0.68 mL, 3.88 mmol). Compound A (0.978 g, 2.59 mmol), dissolved in THF (20 mL), was then added dropwise under magnetic stirring which was continued for an additional 2 h after addition at 0°C . After warming to room temperature, THF was removed under reduced pressure and the residue was partitioned between CH_2Cl_2 and 1 N HCl. The organic layer was washed with H_2O and dried over MgSO_4 . The solvent was removed under vacuum and the resulting solid was purified by column chromatography (SiO_2 ; $\text{CH}_2\text{Cl}_2/\text{MeOH}$ 10/0.25) to afford compound **1** as a white solid in 83% yield. MP: $118\text{--}119^\circ\text{C}$. ^1H NMR (CDCl_3 , 400 MHz): 3.42 (t, 4H); 3.69 (t, 4H); 5.06 (s, 4H); 7.33 (m, 10H). ^{13}C NMR (CDCl_3 , 400 MHz): 38.99, 48.64, 66.85, 128.20–128.34–136.25, 156.56, 165.62, 170. HRMS (ESI+): calcd for $\text{C}_{23}\text{H}_{25}\text{N}_6\text{O}_4\text{Cl}_2$ ($M + H$), 519.1314; found, 519.1306.

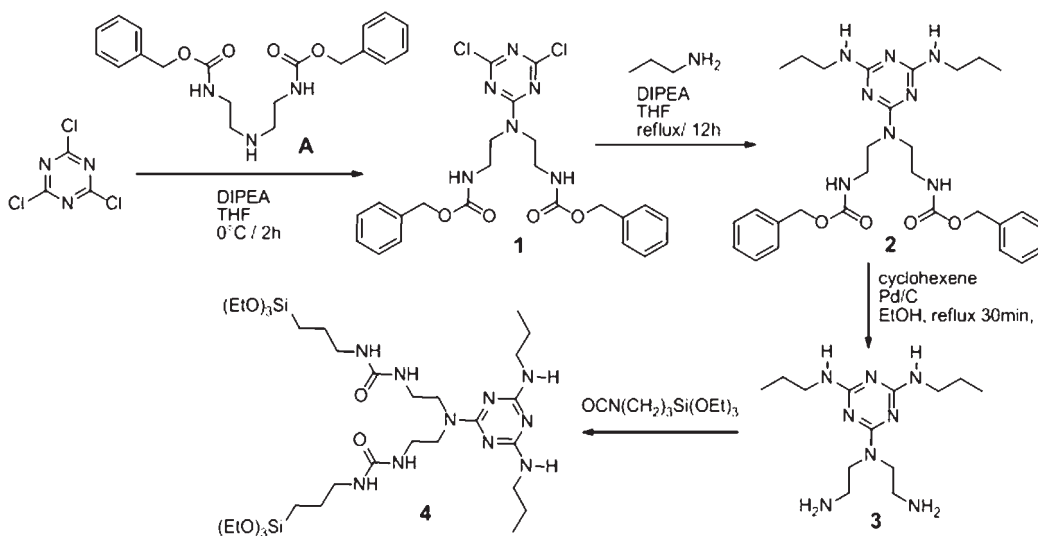
Compound **2** (*2-N,N-bis(2-Cbz-Aminoethyl)amino-4,6-bis(N-propylamino)-1,3,5-triazine*). Propylamine (1.52 mL, 18.45 mmol) and compound **1** (0.96 g, 1.85 mmol) were refluxed in THF (30 mL) overnight. After concentration under reduced pressure, the resulting oil was dissolved in CH_2Cl_2 . The organic layer was washed with H_2O and dried over MgSO_4 . The solvent was removed under vacuum to give quantitatively compound **2** as a colorless oil. ^1H NMR (CDCl_3 , 400 MHz): 0.87 (t, 6H); 1.49 (m, 4H); 3.26 (t, 4H); 3.39 (t, 4H); 3.66 (t, 4H); 4.74 (s, 2H); 5.06 (s, 4H); 6.31 (s, 2H); 7.31 (m, 10H). ^{13}C NMR (CDCl_3 , 400 MHz): 11.0, 22.5, 40.4, 42.0, 46.1, 65.9, 127.5, 128, 136.4, 156.3, 165.1. HRMS (ESI+): calcd for $\text{C}_{29}\text{H}_{41}\text{N}_8\text{O}_4$ ($M + H$), 565.3251; found, 565.3255.

Compound **3** (*2-N,N-bis(2-Aminoethyl)amino-4,6-bis(N-propylamino)-1,3,5-triazine*). To a solution of compound **2** (0.919 g, 1.63 mmol) in EtOH (40 mL) was added cyclohexene (4 mL) and Pd/C (0.23 g, 1/4 equiv per weight). The mixture was refluxed for 30 min and filtered through Celite. EtOH was removed under reduced pressure and the resulting oil was purified by column chromatography (SiO_2 ; $\text{CH}_2\text{Cl}_2/\text{MeOH}$ 8/2 and then $\text{CH}_2\text{Cl}_2/\text{MeOH}/\text{NH}_4\text{OH}$ 8/2/0.33). Compound **3** was obtained as an off-white solid in 81% yield. MP: $69\text{--}71^\circ\text{C}$. ^1H NMR (CDCl_3 , 400 MHz): 0.89 (t, 6H); 1.50 (m, 4H); 2.88 (t, 4H); 3.24 (t, 4H); 3.56 (t, 4H); 4.90 (s, 2H). ^{13}C NMR (CDCl_3 , 400 MHz): 11.4, 23.0, 40.5, 42.4, 50.0, 165.9. HRMS (ESI+): calcd for $\text{C}_{13}\text{H}_{29}\text{N}_8$ ($M + H$), 297.2515; found, 297.2513.

Compound **4**. In a Schlenk tube, compound **3** (1.35 g, 4.55 mmol), anhydrous CH_2Cl_2 (30 mL), triethylamine (1.4 mL, 10.01 mmol) and 3-isocyanatopropyltriethoxysilane (2.5 mL, 10.01 mmol) were stirred overnight under nitrogen. After removal of CH_2Cl_2 under reduced pressure, the resulting white solid was washed with dry pentane (3 times, 50 mL). Compound **4** was obtained in 70% yield as a white solid. MP: decomposition. ^1H NMR (CDCl_3 , 400 MHz): 0.58 (t, 4H); 0.91 (t, 6H); 1.18 (t, 18H); 1.54 (m, 8H); 3.06 (q, 4H); 3.27 (m, 4H); 3.41 (m, 4H); 3.60 (m, 4H); 3.78 (q, 12H). ^{13}C NMR (CDCl_3 , 400 MHz): 0.9, 7.5, 11.4, 18.2, 23.0, 23.6, 39.8, 42.5, 42.9, 58.3, 158.8, 165.6. HRMS (ESI+): calcd for $\text{C}_{33}\text{H}_{71}\text{N}_{10}\text{O}_8\text{Si}_2$ ($M + H$), 791.4995; found, 791.5006.

Hybrid M1. Compound **4** (0.63 g, 0.699 mmol) and cyanuric acid (34 mg, 0.263 mmol) were completely dissolved in DMSO (2.654 mL) at 50°C . After 1 h, water (172 μL , 9.556 mmol) and NH_4F (64 mL, 0.016 mmol, 0.25 M solution) were added. Spontaneously a white gel was formed and was left under static conditions at room temperature for

Scheme 1. Synthesis of Precursor 4



3 days. After successive washing with water (50 mL), EtOH (100 mL), and acetone (50 mL), a white powder was obtained (400 mg). ^{13}C CP MAS solid state NMR: 11.9, 18.8, 25.2, 43.9, 58.7, 160.4, 164.5. ^{29}Si CP MAS solid state NMR: -66.7, -58.1, -46.4.

Hybrid M0. The same procedure was applied to compound 4 without the cyanuric acid, yielding M0 as a white powder. In this case, the gel was formed only after cooling to room temperature. ^{13}C CP MAS solid state NMR: 12.1, 24.0, 43.2, 160.4, 166.7. ^{29}Si CP MAS solid state NMR: -67.0, -58.4.

Hybrid M2. Material M1 (816 mg) was suspended in EtOH (164 mL) and HCl (139 μL , 10^{-2} M) and heated under reflux with stirring for 24 h. The material was filtered and washed several times with ethanol, yielding a white powder. The latter was then treated with aqueous Et₃N (85 mL of water, 8.4 mL of Et₃N) and stirred overnight to neutralize the protonated N-H so as to recover the original DAD center of the triazine fragment. After filtration and washing with EtOH, M2 was obtained as a white powder. ^{13}C CP MAS solid state NMR: 11.9, 18.8, 23.8, 43.2, 58.7, 160.6, 166.7. ^{29}Si CP MAS solid state NMR: -66.3, -61.7.

RESULTS AND DISCUSSION

Synthesis of the bis-Silylated Triazine Precursor 4. Precursor 4 was synthesized in four steps (Scheme 1) from cyanuric chloride via stepwise substitution of the three chloro substituents by either a primary or a secondary amine.³³ In the first step, cyanuric chloride was reacted with 1.0 equiv of A bearing two CBz protecting groups³⁴ at 0 °C in the presence of *N,N*-diisopropylethylamine (DIPEA) in THF, which yielded 1 in 83% yield. In a second step the *N,N',N'',N'''*-tetraalkyltriazine derivative 2 was then obtained in quantitative yield by reacting 1 with an excess of propylamine at 90 °C in THF. Subsequent CBz deprotection was realized using cyclohexene with Pd/C in ethanol under reflux for 30 min, to give compound 3 in 81% yield. The two deprotected primary amino groups of compound 3 were then reacted, under inert atmosphere, with 3-isocyanatopropyltriethoxysilane (2 equiv) to give the targeted silylated precursor 4 in 70% yield. The CBz groups thus protect the two primary amines in the first step of the synthesis, and hence selectively direct substitution at the secondary amine. Subsequent deprotection of the primary amines would then allow silylation with an isocyanate in the subsequent

step. For convenience (easy handling and purification of the non moisture-sensitive intermediates 1–3), silylation was chosen as the last step of the synthesis pathway.

Preparation of the Imprinted Bridged Silsesquioxane. Three hybrid materials were obtained for our study: M0, M1 and M2 (Figures 2 and 3).

To design the imprinted hybrid material M1, the bis-silylated precursor 4 (one DAD face) was complexed with cyanuric acid AC (three ADA faces) in hot DMSO (Figure 2). Due to the sensitivity of the amino and carbonyl groups of the precursors to protonation and basic conditions, respectively, a nucleophilic catalyst (fluoride anion) was used to ensure the assembly of the two organic units via H-bonding in the resulting hybrid material. The two organic compounds were dissolved in hot DMSO and hydrolysis—condensation was initiated by adding water and ammonium fluoride as a catalyst. A gel was formed spontaneously and was aged under static conditions at room temperature for 3 days to afford, after filtration, washing, and drying, M1 as a white powder. M2 was obtained from M1 by treating the latter with boiling acidic ethanol solution (10^{-2} M HCl in EtOH) for 24 h to remove cyanuric acid (Figure 2).

For comparison, a blank experiment M0 was carried out under the same conditions without using cyanuric acid as template (Figure 3). In this case, gel formation was also observed, but only after cooling the reaction mixture to ambient temperature.

Scanning Electron Microscopy (SEM) Studies. SEM images of M0 revealed a spherical morphology with a heterogeneous distribution of particle sizes (Figure 4A) ranging from 1 to 70 μm . In addition, nanoparticles (150 and 300 nm) were also observed (Figure 4B). In contrast, SEM images of M1 (Figure 4C) exhibit a completely different morphology. Indeed, nanometer-size and fiber-like structures, entangled together to form a macroporous network are observed (width 100 nm). This provides clear evidence that the templating and imprinted cyanuric molecules significantly influence the shape of the resulting material and reflects the strong H-bonding interaction between the two complementary fragments (DAD–ADA, respectively, from triazine–cyanuric acid). Interestingly, these shapes are well preserved in M2 (Figure 4D), after complete removal of cyanuric

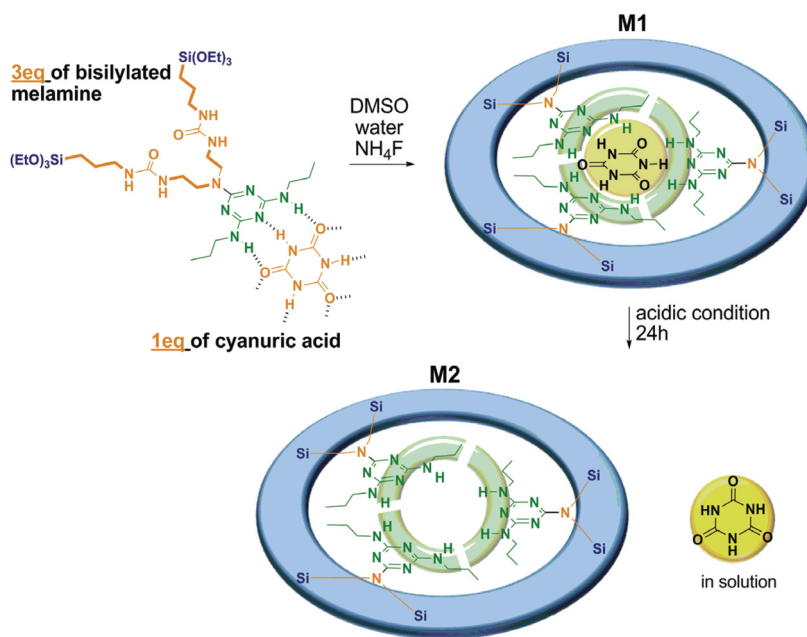


Figure 2. Preparation of M1 and M2.

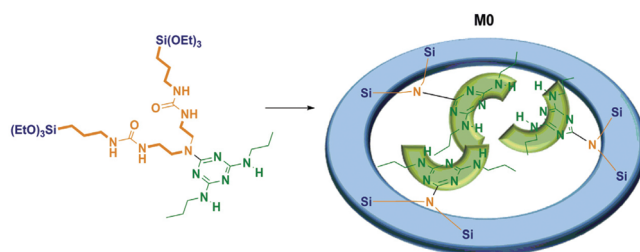


Figure 3. Preparation of M0.

acid by strong pH treatment ($\text{pH} = 2$) which demonstrates the robustness of the material.

Thermal Analyses. The TGA analysis of **M0** is consistent with the decomposition of the material in a single step commencing at around 250°C (Figure 5A). At lower temperature, in the range 100 – 200°C , loosely bound water molecules are desorbed. At 300°C , the material decomposes in a very narrow temperature range, consistent with the synthesis route of the material which was prepared from a simple bis-silylated precursor without any templating agent or mineralizing species such as TEOS. From the weight loss observed at 500°C , it can be deduced that **M0** is composed of $\sim 75\%$ of organics.

The TGA curve associated with **M1** in which cyanuric acid is present is more complex, and several weight losses can be observed between 100 and 300°C (Figure 5B). This indicates that the material is heterogeneous, confirming the presence of cyanuric acid in its framework. The weight loss at low temperature (100 – 150°C) exhibits a trend similar to that observed for **M0**, corresponding to the loss of water (3.5–4.5%). However, in the region 200 – 250°C , there is a clear difference with a significant weight loss in the case of **M1**. This is attributed to the removal of the loosely H-bonded cyanuric acid moieties and is consistent with the cyanuric acid/3 bis-silylated precursor molar ratio.

The main weight loss corresponding to the decomposition and the removal of the bis-silylated condensed precursor has the same

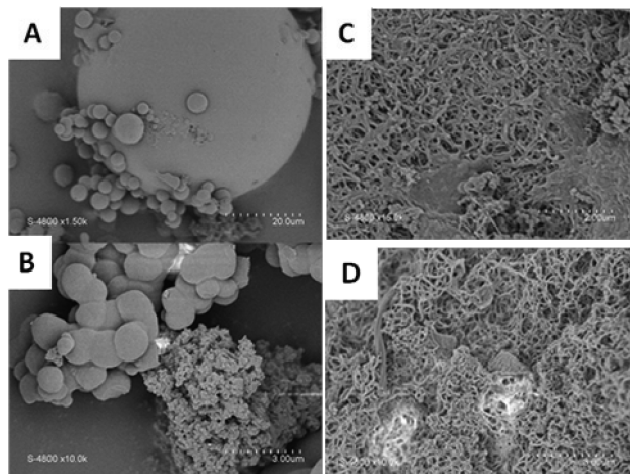


Figure 4. SEM images of (A) and (B) M0, (C) M1 and (D) M2.

extent in both cases ($\sim 55\%$). However, the weight loss is not as steep in the case of **M0** which suggests that cyanuric acid moieties destabilize the bis-silylated condensed precursor.

Figure 5C illustrates the decomposition of **M2**. The TGA curve obtained with this material is very similar to the one found in the case of **M0**, which is consistent with the hypothesis that the cyanuric acid has been removed in **M2**. More explicitly, it can be deduced that the acidic conditions employed are efficient enough to remove the cyanuric acid moieties from the structure.

These experiments are consistent with the textural characterization of the materials showing that the synthesis of the cyanuric acid/bis-silylated precursor has been successfully achieved. More interestingly, these data also show that despite host/guest interaction strong enough to retain the guest within the hybrid material, an acidic treatment is adequate to remove the cyanuric moieties without breaking down the structure, allowing for structured cavities to be created within the framework of the material.

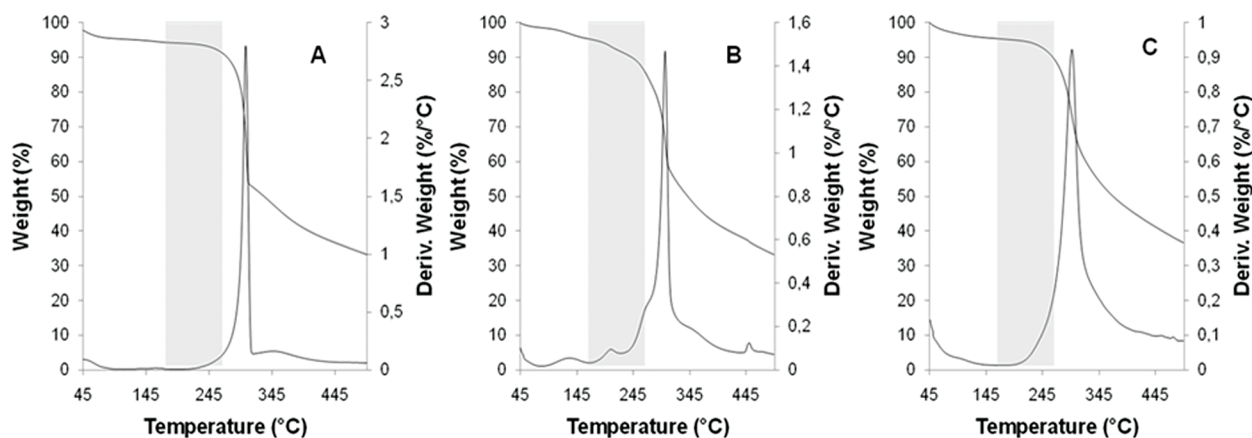


Figure 5. TGA analysis of (A) M0, (B) M1, and (C) M2.

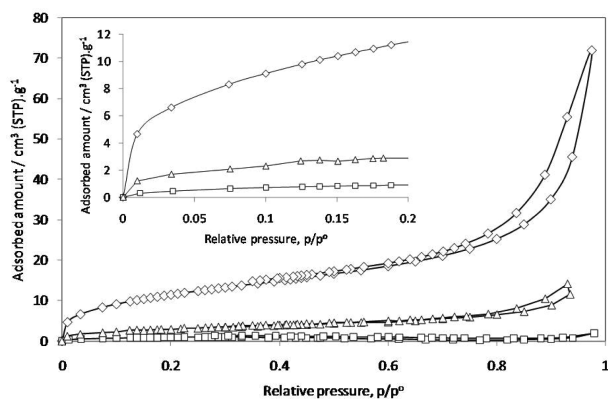


Figure 6. Discontinuous sorption isotherms of nitrogen for M0 to M2.

Textural Properties of the Different Materials. Figure 6 shows the nitrogen adsorption isotherms of the various samples. Essentially no sorption was evident in the case of M0 (squares) made from the precipitation of hybrid silica precursors. In terms of textural properties, this can be attributed to the presence of a non porous material made of large aggregated and condensed particles of the bis-silylated precursor (M0). This sorption isotherm confirms that a template is required to improve the textural properties of the condensed bis-silylated precursor. If the template is present during the preparation of the material, a different adsorption isotherm is found (triangles, M1). In this case, some N_2 sorption is evident, although the extent of sorption is still limited indicating that the majority of cavities are filled by the template and N_2 is sorbed mainly on the external surface of the particles. These can be seen by SEM (Figure 4C). Indeed, it is important to note that the as-synthesized M1 probably does not sorb any nitrogen within the internal cavities, which implies that the structure of the cyanuric acid/bis-silylated precursor is relatively dense. In contrast, the sorption isotherms for M2 (Figure 6) are consistent with significant uptake of N_2 ; this, together with the relatively steep slope in the isotherm at zero N_2 coverage and a specific surface area of around $45 \text{ m}^2 \cdot \text{g}^{-1}$ confirm that the textural properties of the material have changed. From the SEM images (Figure 4D), it can be seen that the acid treatment left the particle size essentially unchanged, which suggests that the increase in specific surface area cannot be related to a decrease in the size of the particles between M1 and M2. It is therefore clear

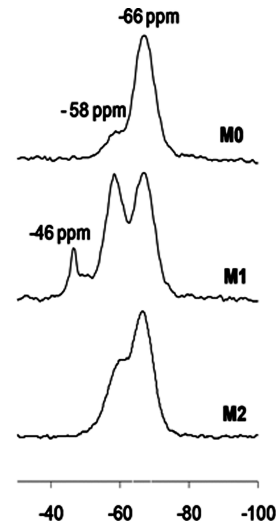


Figure 7. ^{29}Si solid NMR spectra of M0–M2.

that this increase in specific surface area is mostly due to the removal of the template moieties. It can therefore be concluded that an appropriate treatment in acidic conditions (pH 2) generates M2 in which cyanuric acid has been removed, as confirmed by TGA (and NMR and IR studies, as discussed below).

Solid State NMR. The extent of condensation was examined by ^{29}Si solid state NMR (Figure 7). In the case of M0, an intense T3 signal is observed indicating a highly condensed material. The spectrum of M1 exhibits T2 and T3 peaks with similar intensity in addition to a weaker T1 peak consistent with a less condensed material. After the acid treatments of M1 to remove cyanuric acid and generate M2, the intensity of the T3 signal greatly increased, while the T2 signal decreased significantly and the T1 signal was extinguished. Thus the acidic treatment increased the extent of condensation when M1 is transformed to M2. In addition, all the ^{29}Si solid NMR spectra (M0, M1, and M2) showed no Q signal, confirming that the organic components remained covalently bound to the silica network.

The ^{13}C solid state NMR spectra of the three materials confirmed the presence of the bis-silylated triazine fragment (Figure 8). Indeed, in all cases, the spectra exhibited a peak at around 165 ppm characteristic of the triazine $\text{C}_{\text{Ar}}-\text{NH}$, another peak at around 160 ppm assigned to the $\text{C}=\text{O}$ carbon of the urea groups,

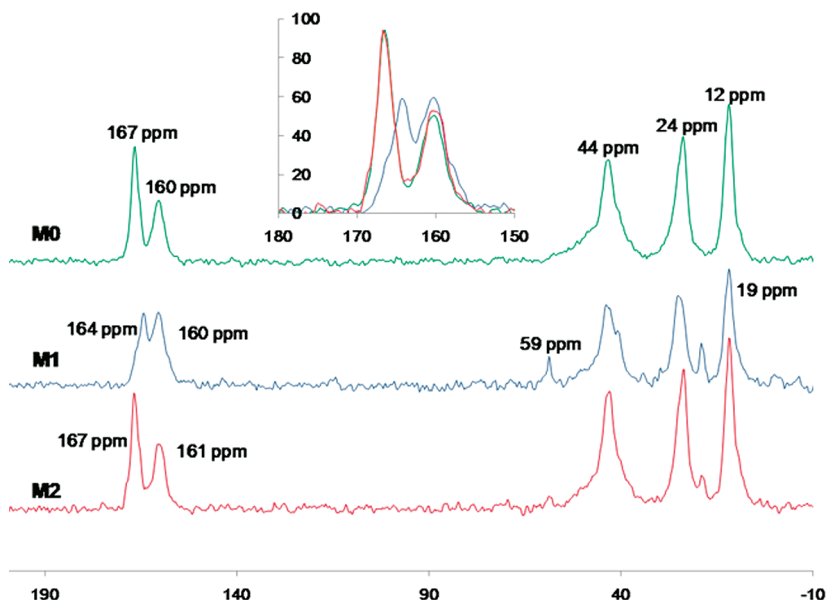


Figure 8. ^{13}C solid NMR spectra of **M0**–**M2**.

and three additional peaks associated with the methylene carbons at 12 ($\text{C}-\text{Si}$), 24 (CH_2), and 44 ($\text{C}-\text{N}$) ppm. The peak at 160 ppm is also characteristic of the $\text{C}=\text{O}$ group of the template molecule (cyanuric acid) which is present only in **M1**. Closer inspection in the range of 150–170 ppm (see inset to Figure 8) indicates two main features:

- a slight shift of the $\text{C}_{\text{Ar}}-\text{NH}$ peak from 167 to 164 ppm is observed in the spectrum of **M1**. This upfield shift is related to the presence of the H-bonding interaction of the anchored triazine unit with the cyanuric acid (absent in **M0** and **M2**).
- the relative intensities of the peaks at 140 to 190 ppm in the spectra of **M0** (green) and **M2** (red) are similar, with the $\text{C}_{\text{Ar}}-\text{NH}$ at 167 ppm being more intense than the $\text{C}_{\text{urea}}=\text{O}$ in both cases. In contrast, the corresponding peaks exhibit comparable intensities in **M1** (blue) resulting from the presence of the additional $\text{C}=\text{O}$ group of the template cyanuric acid. The similarities of the peaks of **M0** and **M2** and the downfield shift of the $\text{C}_{\text{Ar}}-\text{NH}$ peak to 167 ppm in **M2** at exactly the same chemical shift found in **M0** indicate the absence of cyanuric acid in both materials.

Solid FTIR Spectroscopic Analyses. The FTIR spectrum of the precursor **4** exhibits two absorption bands at 984 and 1092 cm^{-1} characteristic of $\text{Si}-\text{O}-\text{C}_2\text{H}_5$ vibrations (Figure 9). The intensity of these bands either decreases (1092 cm^{-1}) or completely disappears (984 cm^{-1}) during hydrolysis, yielding two broad bands (centered at 1100 and 1020 cm^{-1}) attributable to siloxane bridges ($\text{Si}-\text{O}-\text{Si}$) in the spectra of the hybrid materials (**M0**, **M1**, and **M2**).^{35,36} Interestingly, the band at 1100 cm^{-1} is more intense for **M0** indicating a higher degree of condensation²⁸ in this material as observed by solid state ^{29}Si NMR. Moreover, a sharp peak at 810 cm^{-1} assigned to a vibration of the triazine ring³⁷ is also observed in every spectrum, which further confirms the presence of the triazine fragment in the precursor **4** and the materials **M0**, **M1**, and **M2**.

Infrared spectroscopy is an appropriate tool to inspect the presence/absence of the template molecule provided that at least one of its vibrational modes is distinct from those of the anchored

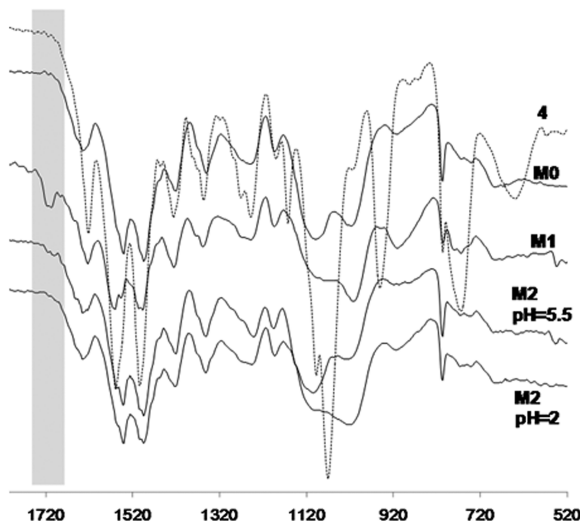


Figure 9. Solid FTIR spectroscopic analysis of compound **4** and materials **M0**–**M2**.

fragments. This is the case in the FTIR spectrum of **M1**, which exhibits a distinct mode at 1720 cm^{-1} corresponding to the $\text{C}=\text{O}$ vibration of the templating cyanuric acid. This band is absent in the FTIR spectrum of **M2** obtained from **M1** after treating the latter with HCl ($\text{pH}=2$). As in our earlier report,²⁴ such treatment under strongly acidic conditions enables the complete removal of cyanuric acid and suggests that the hydrogen bonding interactions between the triazine derivative and the cyanuric acid fragments are suppressed in the material, facilitating the release of the cyanuric acid. It should be noted that the treatment of **M1** with boiling EtOH at neutral pH is not efficient enough to break these H-bonding interactions to remove cyanuric acid. Indeed, no traces of cyanuric acid could be detected in the aliquot even after 24 h. We thus decided to perform further studies at milder pH . Hence treatment of **M1** at $37\text{ }^{\circ}\text{C}$ in an

acetate buffer solution (pH 5.5) was studied. Interestingly, after 24 h stirring, no vibration band is observed at 1720 cm^{-1} in the corresponding infrared spectrum which confirms that this moderate pH treatment is efficient enough to promote the release of the cyanuric acid.

■ CONCLUSION

The first example of a pH-responsive bridged silsesquioxane **M1** obtained from a bis-silylated triazine derivative with an ADA face is reported. This was achieved by the sol–gel hydrolysis–condensation of the precursor in the presence of cyanuric acid H-bonded through the three DAD faces which produced materials with fiber-like morphologies. In contrast, only spherical objects were formed when the bis-silylated precursor was hydrolyzed without cyanuric acid, showing the critical role of the template molecule in modulating the structure of the hybrid material. The template could be easily removed from **M1** upon acid treatment without altering the textural integrity of the material. Furthermore, the functional organic fragments remain covalently bonded to the silica network demonstrating the chemical and thermal stability of the hybrid materials. It was shown that a mild acidic medium (pH = 5.5) is effective in releasing the template from **M1**. This positive and encouraging result is stimulating for further studies in the development of such hybrid materials mainly for examining and creating new efficient carriers for delivery systems.

■ ASSOCIATED CONTENT

S Supporting Information. Figures S1 and S2. This material is available free of charge via the Internet at <http://pubs.acs.org>.

■ AUTHOR INFORMATION

Corresponding Author

*E-mail: carole.carcel@enscm.fr (C.C.) and michel.wong-chi-man@enscm.fr (M.W.C.M.).

■ ACKNOWLEDGMENT

We acknowledge FAME, Ecole Nationale Supérieure de Chimie de Montpellier, and CNRS for financial support. We thank D. Cot (IEM Montpellier) and P. Dieudonné (LCVN Montpellier) for their contribution in the SEM and PXRD measurements, and also J. Bartlett (University of Western Sydney) for fruitful discussions and careful reading of the manuscript. C.T. gratefully acknowledges the “Ministère de l’Enseignement Supérieur et de la Recherche” for a PhD grant.

■ REFERENCES

- (1) Farokhzad, O. C.; Langer, R. *Adv. Drug Delivery Rev.* **2006**, *58*, 1456–1459.
- (2) Caruso, F.; Caruso, R. A.; Moehwald, H. *Science* **1998**, *282*, 1111–1114.
- (3) Fatnassi, M.; Tourné-Péteilh, C.; Cacciaguerra, T.; Dieudonné, P.; Devoisselle, J.-M.; Alonso, B. *New J. Chem.* **2010**, *34*, 607–610.
- (4) Wight, A. P.; Davis, M. E. *Chem. Rev.* **2002**, *102*, 3589–3614.
- (5) Wang, Y.; Bansal, V.; Zelikin, N.; Caruso, F. *Nanoletters* **2008**, *8*, 1741–1745.
- (6) Son, S. J.; Reichel, J.; He, B.; Schuchman, H.; Lee, S. B. *J. Am. Chem. Soc.* **2005**, *127*, 7317–7317.
- (7) Kresge, C. T.; Leonowicz, M. E.; Roth, W. J.; Vartulli, J. C.; Beck, J. S. *Nature* **1992**, *359*, 710–712.
- (8) Huo, Q.; Margolese, D. I.; Ciesla, U.; Feng, P.; Gier, T. E.; Sieger, P.; Leon, R.; Petroff, P. M.; Schüth, F.; Stucky, G. D. *Nature* **1994**, *368*, 317–321.
- (9) Bagshaw, S. A.; Prouzet, E.; Pinnavaia, T. J. *Science* **1995**, *269*, 1242–1244.
- (10) Burkett, S. L.; Sims, S. D.; Mann, S. *Chem. Commun.* **1996**, 1367–1368.
- (11) Macquarrie, D. J. *Chem. Commun.* **1996**, 1961.
- (12) Lim, M. H.; Blanford, C. F.; Stein, A. *J. Am. Chem. Soc.* **1997**, *119*, 4090.
- (13) Sanchez, C.; Julian, B.; Belleville, P.; Popall, M. *J. Mater. Chem.* **2005**, *15*, 3559–3592.
- (14) Coti, K. K.; Belowich, M. E.; Liang, M.; Ambrogio, M. W.; Lau, Y. A.; Khatib, H. A.; Zink, J. I.; Khashab, N. M.; Stoddart, J. F. *Nanoscale* **2009**, *1*, 16–39.
- (15) Zamboulis, A.; Moitra, N.; Moreau, J. J. E.; Cattoën, X.; Wong Chi Man, M. *J. Mater. Chem.* **2010**, *20*, 9322–9338.
- (16) Shimojima, A.; Kuroda, K. *Chem. Rec.* **2006**, *6*, 53–63.
- (17) Carlos, L. D.; de Zea Bermudez, V.; Amaral, V. S.; Nunes, S. C.; Silva, N. J. O.; Ferreira, R. A. S.; Rocha, J.; Santilli, C. V.; Ostrovskii, D. *Adv. Mater.* **2007**, *19*, 341–348.
- (18) Inagaki, S.; Guan, S.; Oshuna, T.; Terasaki, O. *Nature* **2002**, *416*, 304–307.
- (19) Asefa, T.; MacLachlan, M. J.; Coombs, N.; Ozin, G. A. *Nature* **1999**, *402*, 867.
- (20) Chevalier, P. M.; Corriu, R. J. P.; Moreau, J. J. E.; Wong Chi Man, M. *J. Sol-Gel Sci. Technol.* **1997**, *8*, 603–607.
- (21) Chevalier, P. M.; Corriu, R. J. P.; Delord, P.; Moreau, J. J. E.; Wong Chi Man, M. *New J. Chem.* **1998**, *22*, 423–433.
- (22) Marx, S.; Avnir, D. *Acc. Chem. Res.* **2007**, *40*, 768–776.
- (23) Glad, M.; Norrällöw, O.; Sellergren, B.; Siegbahn, N.; Mosbach, K. *J. Chromatogr. A* **1985**, *3437*, 11–23.
- (24) Fireman-Shores, S.; Popov, I.; Avnir, D.; Marx, S. *J. Am. Chem. Soc.* **2005**, *127*, 2650–2655.
- (25) Burleigh, M. C.; Dai, S.; Hagaman, E. W.; Lin, J. S. *Chem. Mater.* **2001**, *13*, 2537–2546.
- (26) Arrachart, G.; Carcel, C.; Trens, P.; Moreau, J. J. E.; Wong Chi Man, M. *Chem. Eur. J.* **2009**, *15*, 6279–6288.
- (27) Shea, K. J.; Loy, D. A.; Webster, O. W. *J. Am. Chem. Soc.* **1992**, *114*, 6700–6710.
- (28) Corriu, R. J. P.; Moreau, J. J. E.; Thépot, P.; Wong Chi Man, M. *Chem. Mater.* **1992**, *4*, 1217–1224.
- (29) Moreau, J. J. E.; Pichon, B. P.; Arrachart, G.; Wong Chi Man, M.; Bied, C. *New J. Chem.* **2005**, *29*, 653–658.
- (30) Arnal-Herault, C.; Barboiu, M.; Petit, E.; Michau, M.; Van der Lee, A. *New J. Chem.* **2005**, *29*, 1535–1539.
- (31) Rouquerol, F.; Rouquerol, J.; Sing, K. In *Adsorption by Powders and Porous Solids*; Academic Press: New York, 1999.
- (32) Trens, P.; Russell, M. L.; Spjuth, L.; Hudson, M. J.; Liljenzin, J. O. *Ind. Eng. Chem. Res.* **2002**, *41*, 5220–5225.
- (33) Arduini, M.; Crego-Calama, M.; Timmerman, P.; Reinhoudt, D. N. *J. Org. Chem.* **2003**, *68*, 1097–1106.
- (34) Pittelkow, M.; Lewinsky, R.; Christensen, J. B. *Synthesis* **2002**, *15*, 2195–2202.
- (35) Bantignies, J.-L.; Vellutini, L.; Maurin, D.; Hermet, P.; Dieudonné, P.; Wong Chi Man, M.; Bartlett, J. R.; Bied, C.; Sauvajol, J.-L.; Moreau, J. J. E. *J. Phys. Chem. B* **2006**, *110*, 15797–15802.
- (36) Innocenzi, P. *J. Non-Cryst. Solids* **2003**, *316*, 310–319.
- (37) Kimizuka, N.; Kawasaki, T.; Hirata, K.; Kunitake, T. *J. Am. Chem. Soc.* **1998**, *120*, 4094–4104.